Rapid Prototyping of Functional Three-Dimensional Microsolenoids and Electromagnets by High-Pressure Laser Chemical Vapor Deposition

J. Maxwell,[†] K. Larsson, M. Boman
Dept. of Inorganic Chemistry, Ångström Laboratory, Uppsala Univ., Uppsala, Sweden

P. Hooge, Kirk Williams, P. Coane
Institute for Micromanufacturing, Louisiana Tech Univ., 911 Hergot Ave., Ruston, LA, USA

High field-density microsolenoids from 100 to 500 microns in diameter were prototyped using both low and high pressure laser chemical vapor deposition. Tungsten lines were drawn about coated Co-Fe-Si-B magnetic cores from a mixture of WF_6 and hydrogen, yielding prototype microelectromagnets. Free-standing tungsten carbide coils and single crystal tungsten needles were deposited at high deposition rates from a variety of WF_6-H_2-He mixtures. The WF_6-H_2-He system was studied to obtain desired crystal morphologies. The convective cooling and diffusion of Xe vs. He was explored. Carbon fibers and helices were also grown at pressures up to 3000 mbar from ethylene. Peak temperatures during the growth process were monitored continuously with a simple apparatus which will be described. The future of high-pressure LCVD for micro-scale rapid prototyping of metals appears to be promising.

Keywords: Laser Deposition, Tungsten, Carbon, Direct-writing, Freeform Growth, Microsolenoid, Microelectromagnet, Microcoils, Microsprings, Probes

I. Introduction

Three-dimensional laser chemical vapor deposition (3D-LCVD) is an emerging process which bridges the gap between various macro-scale rapid prototyping (RP) systems and microfabrication technologies. With the ability to deposit both metals and dielectrics 3D-LCVD may be used to prototype integrated electromechanical components from sub-micron to centimeter scales. This technological niche is increasingly important with the ever-decreasing size and sophistication of consumer and industrial products.

The objective of this work was the development of functional microsolenoids and electromagnets, using 3D-LCVD as the primary fabrication tool. High-aspect-ratio microsolenoids have the potential to generate much greater magnetic-field densities than their thin-film counterparts,[1] and have many advantages when used as actuators in microelectromechanical systems (MEMS).[2] 3D-LCVD provides a means of fabricating such helical structures, with an ease unparalleled by any lithographic or rapid prototyping process.

II. Method

There are several ways in which 3D-LCVD can be used to generate a microcoil. The first and simplest method is the direct-writing of a conductive line on an insulated fiber. In this case, the laser beam is focused onto the fiber, normal to the axis of rotation, while the fiber rotates about its axis and is pulled at constant velocity along the axis. This is illustrated in Fig. 1A. The method was first demonstrated with the growth of a tungsten line about a silicon fiber.[3] Note that the fiber itself may also have been previously grown using 3D-LCVD, allowing a complete microsolenoid to be fabricated with one production tool. If the fiber is grown from the gas phase, it can be made to differ in composition from that of the conductive line, merely

[†] Visiting Fellow at Ångström Laboratory

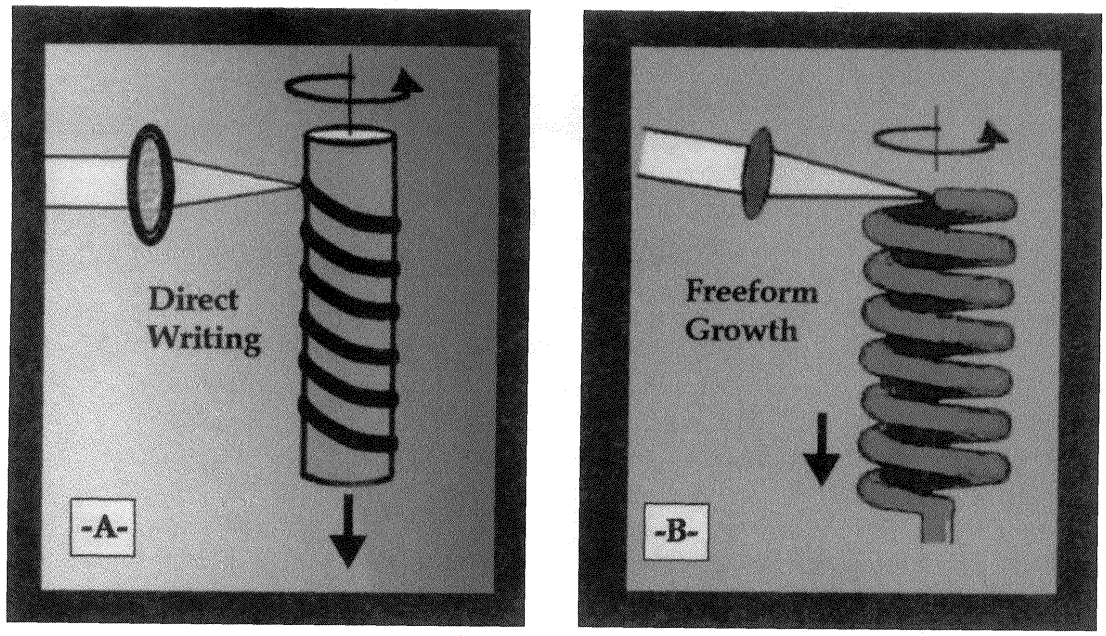

Fig. 1: Techniques for Growing Coils Using 3D-LCVD

by changing the precursor gases.[4] The fiber may also be coated with an insulator from the vapor phase, either by localized direct-writing or large-area heating, so that the conductive line is isolated from the core fiber. In this way, a ferromagnetic material such as iron, nickel, or cobalt (or an alloy of the same) can form the core of an electromagnet, while this core is electrically-insulated from one or more conductive lines by intermediate coatings. Clearly the writing process may be repeated, allowing multiple coils about a single core–with the associated increase in magnetic field strength.

Freeform coils may be grown via 3D-LCVD, as illustrated in Fig. 1B. The laser beam is initially focused on the end of a fiber which is offset from an axis of rotation by the intended helix radius. Once three-dimensional growth initiates, rotation commences about the axis, and the structure is drawn downwards. The tangential velocity of the helix at the focal point, must match (or be slightly less than) the deposition rate, so that the growth front on the tip of the evolving helix appears stationary at the laser focus.

Comparing the convective heat transfer from such a freeform coil to that of a direct-write solenoid, one can see that the freeform coil is more efficient due to the attendant increase in surface area for heat losses. For two coils of identical coil diameter, the freeform coil will have a larger effective surface area by a factor of $\pi\omega N$, where ω is the width of the freeform metal fiber and N is the number of loops per unit length. For a coil diameter of 100 μm, and fiber width of 15 μm, the freeform coil is 5 times more efficient at dissipating heat. In addition, greater currents may be passed through the solid metal fiber than through the thin-film direct-write coil, so much greater magnetic flux densities may be obtained with freeform coils.

The potential to fabricate free-standing microsolenoids using 3D-LCVD was first demonstrated successfully at Uppsala University,[5] with the growth of a free-standing, polycrystalline boron coil. However, a conductive coil which could be used to generate a magnetic field or a flexible coil with adequate mechanical properties had not been realized. The following work describes efforts using both fabrication techniques: direct-writing and freeform growth of metal helices.

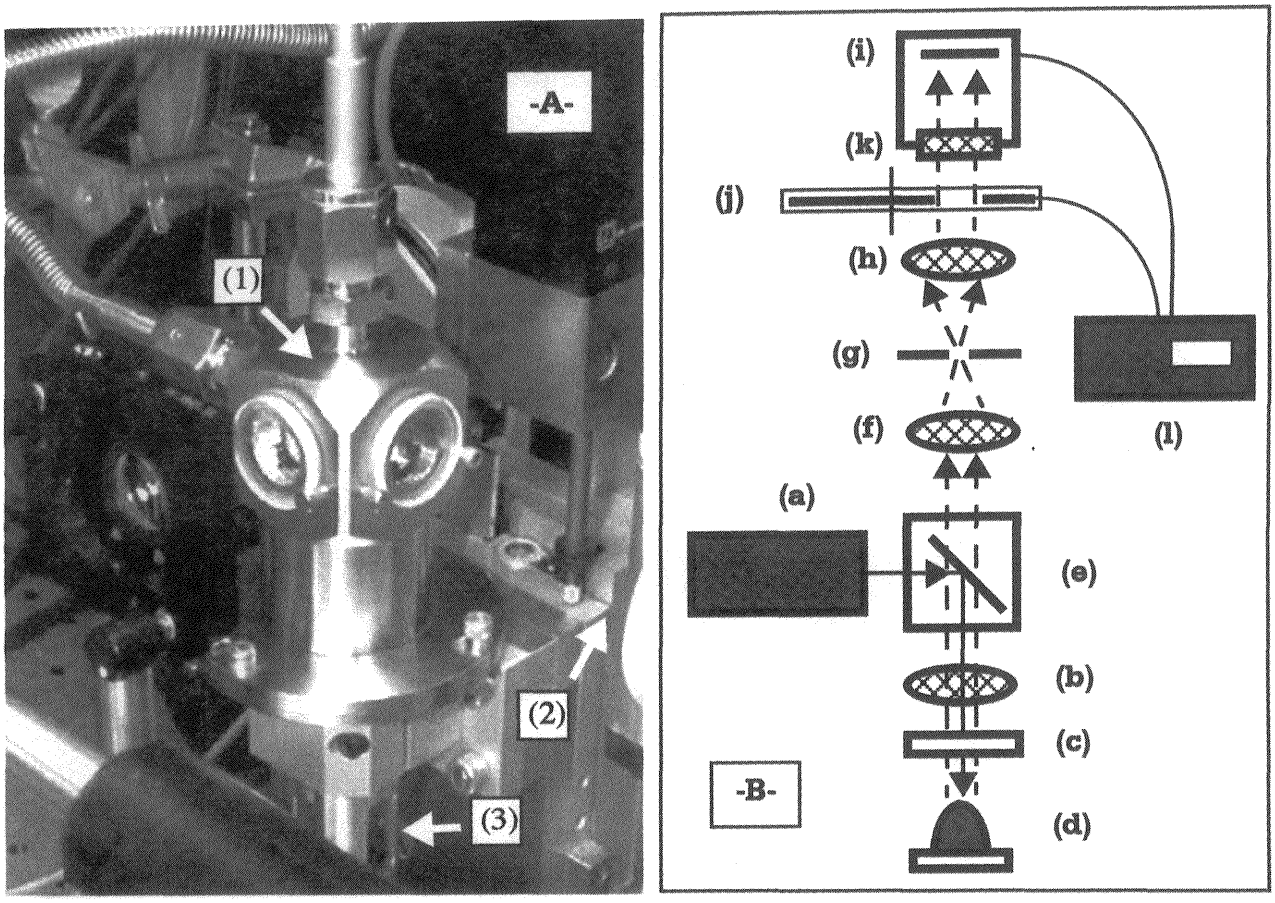

Fig. 2: (A) Pressure Chamber/Stages, (B) Temperature Measurement System

III. Experimental

The 3D-LCVD apparatus shown in Fig. 2A was used for the growth experiments. It consists of a small pressure chamber (1) with two windows, mass flow control system, and vacuum pump with a cold trap. The chamber travels on a Burleigh X-Y-Z stage (2) with piezoelectric actuators, and it is connected to the mass flow control system and vacuum pump with flexible bellows. Repeatability of the stages is greater than 0.1 μm. Rotary motion of the sample is provided by a motion feedthrough (3), driven by a precision DC motor and 1:132,000 planetary gearbox, giving a minimum rotational velocity of 3.0 rph. The sample holder inside the chamber rides on a manual 4-axis goniometer which allows precise alignment of the sample to the feedthrough rotary axis.

The optical system and temperature measurement apparatus is shown in Fig. 2B. A single-mode cw Ar+ laser (a) at 488/514 nm was employed at average powers up to 12 watts, while a 60 mm focal length gradient-index lens (b) was used to focus the beam through a fused- silica window (c) on the chamber, yielding a $1/e^2$ spot waist of approximately 10 μm at the sample (d). Between the laser and focusing lens, a dielectric plate beamsplitter (e) was used to turn the beam by 90°, while passing near infrared wavelengths from 900 to 1500 nm. In this way, it was possible to monitor the emissions and radiation emanating from the center of the growth front.

To measure the peak growth temperature, light passing through the beamsplitter (e) was imaged by an achromat (f) onto a 10 μm or 22 μm diameter pinhole (g), which was carefully centered to obtain maximum throughput. In this way, only light from the center of the growth

zone was allowed to pass–where the peak temperature (and brightest signal) would be observed. This also simplified the temperature measurement, so that a local micro-scale temperature could be inferred, rather than an average temperature over the growth front. A relay lens (h) was then used to concentrate the light onto a photodiode (i), through a chopper (j) and narrow band filter (k) with center wavelength at 1100 nm. The chopper frequency selected for all experiments was 142 Hz. The signal from the photodiode was passed into a current preamp, then into a lock-in amplifier (l) to eliminate noise. This simple temperature measurement system works with a signal-to-noise ratio of over 25 dB, and is able to accurately detect temperatures to within ±10°C, which is sufficient to avoid melting of the deposit during transient growth and adequate for rudimentary growth rate control in the kinetically-limited regime.

For the deposition of tungsten, the precursor tungsten hexafluoride, WF_6, was employed in various ratios to hydrogen, which acts as a reducer. The overall deposition reaction was:

$$WF_6 + 3H_2 \rightarrow W_{(s)} + 6HF. \quad (1)$$

Tungsten hexafluoride is a liquid at room temperature, with a vapor pressure of approximately 800 mbar. Hot air guns were directed at the chamber windows, and run continuously, to eliminate condensation (and deposition) on the windows. It was found that pre-heating the windows under vacuum to 100°C for 15-20 minutes prior to the introduction of WF_6 greatly reduced the probability of adsorption and condensation on the windows, presumably due to desorption of all water on the window surfaces.

Competition between deposition and etching was also observed on the boron substrates. Boron may be etched by both hydrogen and fluorine; the reaction:

$$2B_{(s)} + 3H_2 \rightarrow 2BH_3 \quad (2)$$

dominates if the relative hydrogen concentration is high, while:

$$2B(s) + 3F_2 \rightarrow 2BF_3 \quad (3)$$

is dominant if the relative concentration of WF_6 is high. Thus, it was necessary to balance the molar ratio of H_2/WF_6 to eliminate etching. A variety of hydrogen to WF_6 ratios were attempted from 1:5 to 10:1.

Tungsten carbide was also grown using a mixture of WF_6, H_2, and ethylene, C_2H_4. A stochiometric mix was employed to obtain the intermetallic WC:

$$2WF_6 + C_2H_4 + 4H_2 \rightarrow 2WC_{(s)} + 12HF. \quad (4)$$

As the tungsten hexafluoride threshold temperature for decomposition is approximately 300°C in the presence of H_2, while that for ethylene is over 800°C, ethylene is not necessarily an ideal precursor. To compensate for the tendency to grow tungsten-rich deposits, greater ethylene concentrations were also investigated, as well as deposition temperatures over 1000°C.

IV. Results

A) Direct-write Microsolenoids

To fabricate microsolenoids using the direct-write technique, 100 μm boron fibers were carefully aligned with the axis of rotation of the motion feedthrough described above, and the laser focus was aligned to the center of the fiber. Tungsten was successfully deposited on these boron fibers at a variety of scan rates and precursor partial pressures. The best results to date were obtained with a 1:4 mixture of WF_6 to H_2 at 100 mbar. The laser power employed was 180 mW. Fig. 3 shows an example of a microsolenoid grown under these conditions. Note that the lines are well-defined and nearly flat, the tungsten grain sizes are less than 1-2 microns,

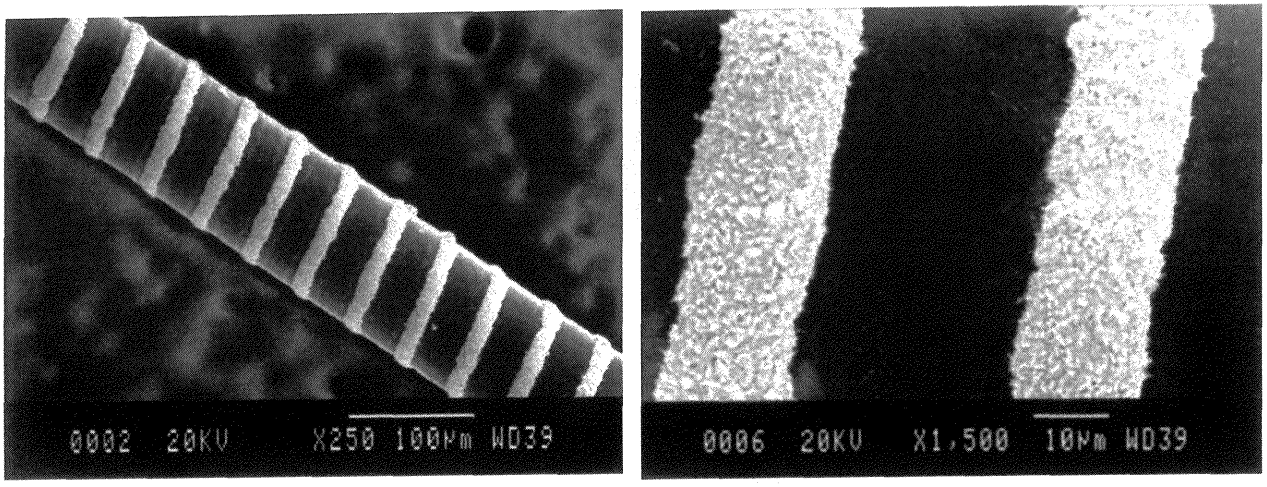

Fig. 3: Tungsten on Boron Microsolenoid by Laser Direct-writing

and there is little deposition of tungsten or etching of boron between the lines. Average central line thickness was 3 μm.

The thickness of the tungsten lines was found to be inversely proportional to the scan rate, while the width of the lines was approximately the same as the spot size (10-15 μm) over a wide range of scan rates, but broadened as the scan rate approached zero velocity, reducing the resolution of the helix and number of possible turns per unit length. In addition, it was noted that increasing overall pressure tended to increase the deposition rate and reduce the grain size of the tungsten deposit. So, to maintain consistent results and high definition lines, the scan rate had to be raised as the pressure was increased.

In addition to the boron-core microsolenoids, tungsten was also deposited on 100 μm diameter Co-Fe-Si-B alloy fibers. To insulate the core from the tungsten coil, the fibers were CVD-coated with a 1-2 μm thick silicon layer using a silane and hydrogen ambient and resistive heating of the Co-alloy fibers. The adhesion of the silicon coating to the Co-alloy fibers was adequate. Tungsten could be readily grown on these fibers, as in the case of the boron-core microsolenoids, although higher laser powers, on the order of 500 mW, were required to compensate for the thermal conductivity of the Co-alloy, and the Si coating was readily etched, leaving the metal lines uninsulated. Ongoing efforts are being made to substitute a boron coating for the silicon, so that these microelectromagnets may be fully tested.

B) Free-standing Microsolenoids

As a basis for comparison and because of its outstanding mechanical properties and favorable microstructure, carbon was selected as the preliminary deposit material for growing free-standing microcoils, since the 3D-LCVD of amorphous carbon rods from ethylene has been previously characterized.[6] As described earlier, functional microsolenoids could also be fabricated using the carbon helices as cores, or the carbon could be used as a sacrificial layer in the production of microtubes.

Again, boron fibers were used as the substrates, aligned to the rotary feedthrough axis. Ethylene was introduced at pressures between 400 and 3000 mbar, and laser powers between 150 mW and 1200 mW provided a variety of carbon fiber diameters. At 930 mbar and 150 mW, smooth, amorphous carbon fibers could be grown with a diameter of only 14 μm. Using these parameters as a basis, several dozen helices were grown, one of which is displayed in Fig. 4. Note that the individual coils could be spaced less than 5 μm apart without affecting

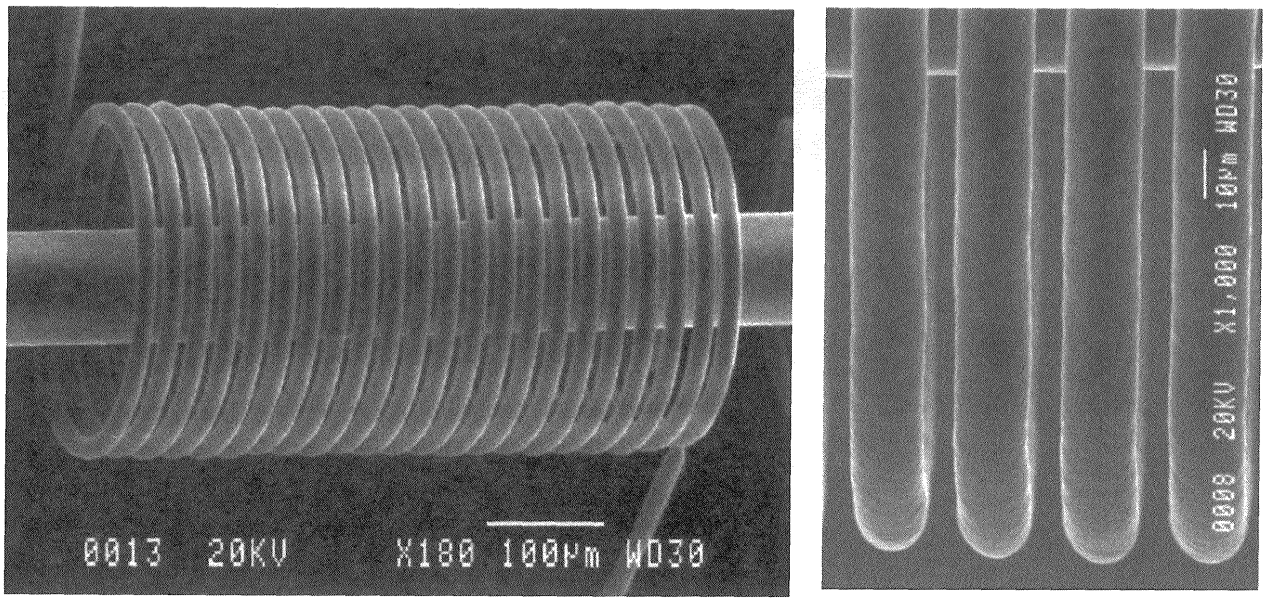

Fig. 4: Amorphous Carbon Microcoils

the shape of the deposit; in fact, it was possible to continuously grow the coils with zero spacing–so that they just barely touch. An attempt was made to grow a tube in this manner, with several microns overlap between coils; in this case, however, heat losses to the adjacent coil were excessive, and the growth became unsteady. Given a 14 μm loop width with 2 μm clear spacing, a metal-coated inductor with over 600 loops per centimeter can be fabricated, more than sufficient to saturate most ferromagnetic cores.[7]

It was also possible to grow very small diameter microcoils of carbon, the smallest to date having a clear internal diameter of only 60 μm. Even smaller diameter solenoids could be prototyped, down to at least 20 μm clear ID, provided the laser spot size is reduced, and a rotary drive and stages with improved resolution were employed. Note that alignment of the focus on the tip of the evolving helix is critical for continual growth. If the helix moves too quickly relative to the focus, either in rotary motion, or along the rotational axis (z-axis), so that the focus is more than a few microns out of place, growth will cease due to reflective losses on the narrow carbon fiber.

Freeform Growth of Tungsten

Using WF_6 and H_2, very rapid growth of free-standing tungsten rods was obtained, up to 160 μm/s continuous rates, and a variety of morphologies were obtained, depending on the laser power and precursor pressure employed. Typical gas mixtures were 3:1 H_2 to WF_6, at chamber pressures from 750 to 3000 mbar. At these pressures, explosive crystal growth would occur using laser powers over 3 W, and rods composed of very large grains would result, or multiple large crystals would grow slowly away from the substrate at various angles to the beam. At lower powers, between 1.5 W and 3.0 W, rods with a single-crystal cores and polycrystalline coatings would form. Within a narrow power range, around 800-900 mW, clean single-crystal, cubic tungsten rods, over 2 mm in length could be grown continuously using focal tracking at rates of over 2 μm/s. These rods were of square cross-section, as shown in Fig. 5A, and could potentially be used as rectangular building blocks in microelectromechanical systems or as wear-resistant probes. At higher pressures, over 1100 mbar chamber pressure, rapid

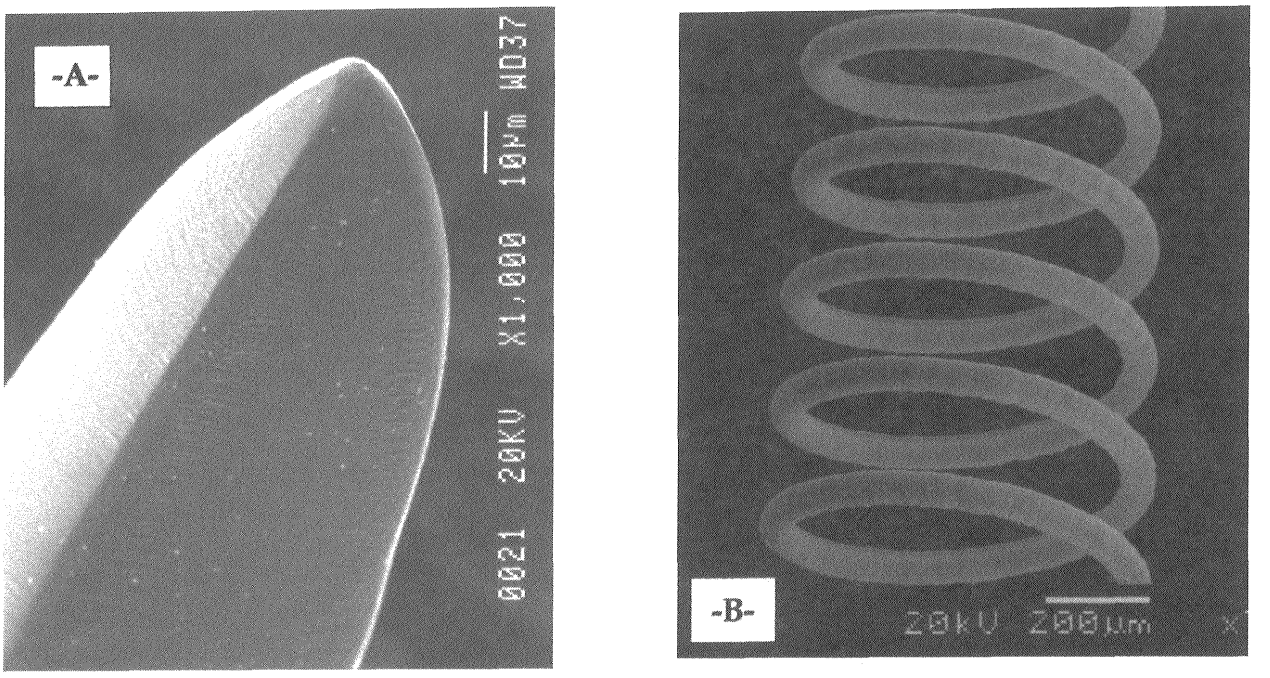

Fig. 5: (A) Tungsten Crystals, (B) Tungsten Carbide Microsolenoid

polycrystalline growth of 10-20 μm/s was obtained, and very narrow rods could be grown, down to about 30 μm in diameter.

It was difficult to obtain circular helices of pure tungsten. Invariably, the growth tended to orient in one direction, and deposition would cease as the angle of incidence to the growth front changed. Precursor pressures greater than 1100 mbar were necessary to produce fine-grained tungsten deposits. Several partial helices were possible, using a chopped beam to induce polycrystalline growth.

Previous papers have studied the influence of convective losses on the ability to grow steady-state metal deposits without self-limiting effects.[8] To compare the losses due to natural convection versus those due to diffusion during steady-state growth, noble gases were also added to the WF_6/H_2 mixture in 50 mbar increments. The temperature was measured using the apparatus described in Fig. 2B. In this case, the base partial pressures of WF_6 and H_2 were 400 mbar and 600 mbar, respectively, and the chamber pressure varied depending on the addition of helium or xenon. A marked cooling effect was noted with the helium mixtures; in one case it was estimated that a 100 mbar increase in helium partial pressure corresponded to additional heat losses of over 100 mW. In addition, heat transport by the helium broadened the transient diameter of the rods, and when over 200 mbar of helium was introduced, homogeneous nucleation in the gas phase commenced near the deposit. As helium has a very high diffusivity, it tends to transport heat rapidly away from the growth front, into the surrounding gas mixture. This, in turn, heats any nearby solid surfaces, and the growth region broadens noticeably. The instantaneous helium concentration in a reactor can thus tailor the growth diameter to follow a specific profile. Experiments were also performed with xenon, which has a gas diffusivity typically 1/6th that of Helium. The deposits grown with Xe were noticeably more well-defined, and homogeneous nucleation was not present even at partial pressures up to 300 mbar.

Purity of the tungsten deposits was examined using energy dispersive x-ray spectroscopy (EDS). No trace of oxygen or fluorine was detected in the deposits, even with H_2:WF_6 flow ratios as low as 1:3.

Freeform Growth of WC Helices

To obtain conductive, freestanding helices, experiments were also performed in the growth of tungsten carbide from a stochiometric mix of WF_6, C_2H_4, and H_2. Again, very rapid continuous growth was obtained, up to 175 μm/s, while the diameter of the fibers was much smaller than that of the pure tungsten samples–as narrow as 20 μm across. Focal tracking was employed to grow fibers as long as 4 mm, with height-to-width aspect ratios of 200:1. The fibers tended to grow in spurts, as hexagonal single-crystals with peak growth rates exceeding 200 μm/s in many instances. Single-crystal deposition rates were so rapid that they were difficult to measure. To obtain polycrystalline deposits, a chopper at 72 Hz was introduced, and smooth, continuous growth at 10-20 μm/s was obtained. In this way, it was possible to change the axial direction of the growth, allowing helices of WC to be prototyped, such as that shown in Fig. 5B. This helix was grown with a 1:2:2 ratio of WF_6:C_2H_4:H_2 at 765 mbar.

Morphology of the tungsten carbide deposits depended strongly on the laser power employed. At the highest powers, several different phases of the W-C system were present, while at low powers, bare hexagonal crystals of WC were obtained. X-ray diffraction studies are currently underway to identify all of the phases. A thin, pure tungsten coating was present on the exterior of many WC structures, due to the differential in threshold decomposition temperatures between WF_6 and C_2H_4. This coating may be readily delaminated, and can be eliminated through the use of low powers, pulsed lasers, or alternate precursors for carbon.

V. Conclusions

Both direct-write and free-standing microsolenoids and electromagnets may be fabricated using 3D-LCVD. Future work will include the incorporation of ferromagnetic materials, the testing and characterization of the resulting microelectromagnets, and their application in microelectromechanical systems (MEMS). Additional studies will be carried out on the effects of noble gases on heat losses during 3D-LCVD, and the deposition of tungsten and tungsten carbide systems will be fully characterized.

VI. Bibliography

1. J.A. Rodgers, R. J. Jackman, G. M. Whitesides, "Constructing Single- and Multiple- Helical Microcoils and Characterizing Their Performance as Components of Microinductors and Microelectromagnets," Journal of Microelectromechanical Systems, Vol. 6, No. 3, Sept. 1997, pp. 184-191.

2. J. Klein, H. Guckel, "High Winding Density Micro Coils for Magnetic Actuators," HARMST '97, Madison, WI, Jun. 1997.

3. H. Westberg, M. Boman, "Free-standing Silicon Microstructures Fabricated by Laser Chemical Processing," J. Appl. Physics, Vol. 73, No. 11, 1 Jun. 1993, pp. 7864-7871.

4. Maxwell, J., Pegna, J., DeAngelis, D., Messia, D., "Three-dimensional Laser Chemical Vapor Deposition of Nickel-Iron Alloys," Material Research Society Symposium Proceedings, v. 397 (B3.30): Advanced Laser Processing, MRS Fall 1995 Meeting, Boston, MA (Nov. 27--Dec.1, 1995).

5. S. Johansson, J. Schweitz, H. Westberg, M. Boman, "Microfabrication of Three-Dimensional Boron Structures by Laser Chemical Processing," J. Appl. Phys., Vol. 72, No. 12, 15 Dec. 1992, pp. 5956-5963.

6. J. Maxwell, "Three-Dimensional Laser-Induced Pyrolysis: Modelling, Growth Rate Control, and Application to Micro-Scale Prototyping," PhD Thesis, Rensselaer Polytechnic Institute, 1996.

7. P. Lorrain, D. Corson, Electromagnetic Fields and Waves, 2nd Edition, Freeman Publ. San Francisco, CA, 1970, pp. 398.

8. Maxwell J., Krishnan, K., "High-Pressure, Convectively-Enhanced, Laser Chemical Vapor Deposition of Titanium," Proc. Solid Freeform Fabrication Symposium, Austin, Texas, Aug. 1997.